

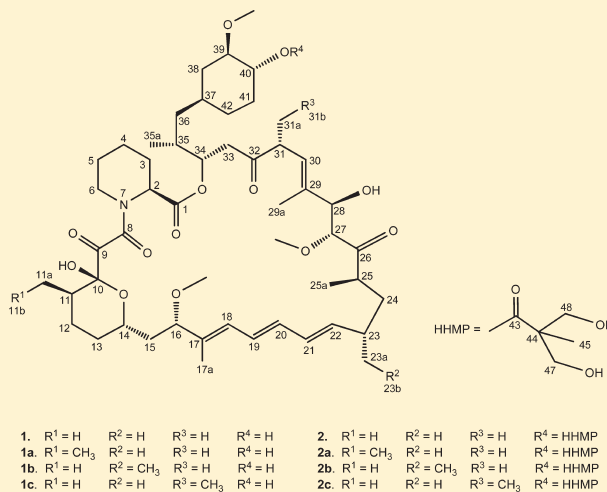
## Isolation and Structure of Homotemsirolimuses A, B, and C

Fangming Kong,\* Tianmin Zhu, Ker Yu, Thomas G. Pagano, Parimal Desai, Galen Radebaugh, and Mahdi Fawzi

Wyeth Research, 401 N. Middletown Road, Pearl River, New York 10965, United States

Supporting Information

**ABSTRACT:** Homotemsirolimuses A, B, and C (**2a**, **2b**, **2c**) were found to be minor components of a temsirolimus preparation made from rapamycin. These three temsirolimus analogues are derived from the corresponding rapamycin analogues, homorapamycins A, B, and C (**1a**, **1b**, **1c**) produced by the strain *Streptomyces hygroscopicus*. The structures of homotemsirolimuses A, B, and C were determined by spectroscopic methods. These compounds were tested for mTOR kinase inhibition and in two proliferation assays using LNCap prostate and MDA468 breast cancer cells. The results suggested that the mTOR inhibition and antiproliferation potencies for **2a**, **2b**, and **2c** are comparable to those of rapamycin (**1**) and temsirolimus (**2**).



Rapamycin (**1**), a 31-membered macrolide, was discovered as a fermentation product of the actinomycete *Streptomyces hygroscopicus* in a soil sample from Easter Island.<sup>1,2</sup> It is the active ingredient in Rapamune, an immunosuppressant drug used to prevent rejection reactions in organ transplantation.<sup>3,4</sup> The mode of action of rapamycin entails binding to the FKBP-12 protein to form a rapamycin–FKBP12 complex that inhibits the mTOR (mammalian target of rapamycin) pathway by direct binding to mTOR complex 1 (mTORC1).<sup>5</sup> Drug-eluting stents containing rapamycin have exploited its antiproliferative effect to prevent restenosis in coronary arteries following balloon angioplasty.<sup>6</sup> The antiproliferative effects of rapamycin may also have a role in treating cancer.<sup>7</sup> In a recent study, the lifespan of mice fed rapamycin was extended up to 38%.<sup>8</sup>

A number of semisynthetic derivatives of rapamycin have been made, most of which involve modification at C-40. Those that are currently in clinical use or under going clinical trials include temsirolimus (CCI-779),<sup>9</sup> everolimus (RAD001),<sup>10</sup> zotarolimus (ABT-578),<sup>11</sup> deferolimus (AP23573),<sup>12</sup> and ILS-920.<sup>13</sup> Temsirolimus (**2**) is made from rapamycin by acylation of the C-40 alcohol (Figure 1). Developed by Wyeth Pharmaceuticals and marketed as Torisel, it has been approved by the FDA and EMEA for the treatment of renal cell carcinoma.

In the development phase of the temsirolimus drug substance, an impurity was found. This late peak, referred to as RRT 1.15 (relative retention time), by reversed-phase HPLC was found to be 14 mass units more than the corresponding temsirolimus API

(active pharmaceutical ingredient). Inspection of the <sup>1</sup>H NMR and <sup>13</sup>C NMR spectra acquired on material representing this late peak revealed that it was a mixture of several structurally related compounds. Multiple cycles of chromatographic separation and purification of the RRT 1.15 peak led to the isolation of three M+14 analogues: homotemsirolimuses A, B, and C (**2a**, **2b**, **2c**). This paper describes the isolation, purification, structure elucidation, and biological activities of the three temsirolimus analogues, **2a**, **2b**, and **2c**.

### RESULTS AND DISCUSSION

**Source and Isolation.** Homotemsirolimuses A, B, and C (**2a**, **2b**, **2c**) were isolated in milligram quantities from a batch of temsirolimus API (batch OM7612) containing a relatively high amount of these compounds (previously designated as the RRT 1.15 impurity). Separation and purification of the compounds were achieved by repeated HPLC separations. The temsirolimus API (2 g) was dissolved in a mixed solvent of acetonitrile and dimethyl sulfoxide, and the solution was then fractionated by preparative reversed-phase HPLC. The column was washed with multiple steps of gradient elution of acetonitrile and water with monitoring by UV detection at 275 nm. Fractions were collected according to peaks or time intervals if no significant UV peak was observed. The obtained samples were analyzed by analytical

Received: May 19, 2010

Published: March 25, 2011

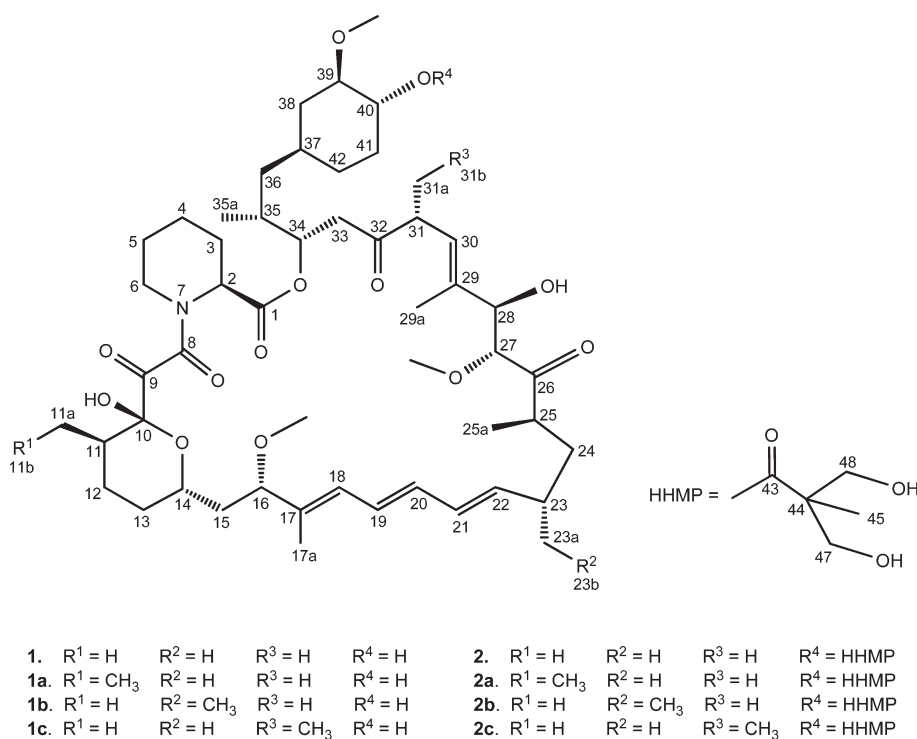


**Figure 1.** Structures of rapamycin (**1**) and minor components homorapamycin A (**1a**), homorapamycin B (**1b**), and homorapamycin C (**1c**); and temsirolimus (**2**) and minor components homotemsirolimus A (**2a**), homotemsirolimus B (**2b**), and homotemsirolimus C (**2c**).

HPLC and/or LC-MS. The fraction collected from 31 to 38 min (Supporting Information) contained the targeted compounds.

The RRT 1.15 impurity-enriched fraction, confirmed by the analytical HPLC method L17677-035, was then chromatographed by semipreparative HPLC to yield a single peak of the RRT 1.15 material (19 mg, Supporting Information). The LC-MS of this sample showed an  $[M - H]^-$  ion peak at  $m/z$  1042.6 and an  $[M + Na]^+$  ion peak at  $m/z$  1066.5, revealing its nominal mass of 1043 Da, 14 more mass units than temsirolimus. However, analysis of the NMR spectra indicated it was a mixture of two major components and a minor one.

The RRT 1.15 sample was subjected to multiple rounds of separation by reversed-phase HPLC. Changing the mobile phase from acetonitrile/water to methanol/water resulted in the separation of the minor component, **2c**, from the major ones, **2a** and **2b**. The separation of **2a** and **2b** was achieved by collection of fractions from the single, wide-eluting peak. LC-MS/MS analysis of these fractions revealed that **2a** was enriched in the front region of the peak and **2b** was enriched in the tail region. Using the acetonitrile/water mobile phase, the elution order of **2a** and **2b** was reversed, although they were still contained in a single chromatographic peak. Repeated recycling of the **2a** and **2b** enriched samples eventually led to the isolation of relatively pure **2a** and **2b**, as judged by  $^1\text{H}$  NMR.

**Structure Determination.** Homotemsirolimus A (**2a**) was prepared as an amorphous, white powder. The UV spectrum was identical to that of temsirolimus, indicating that the extra 14 mass units did not affect the chromophore. The LC-MS analysis of **2a** revealed its molecule related ions at  $m/z$  1066, 1042, and 1088, corresponding to  $[M + Na]^+$ ,  $[M - H]^-$ , and  $[M + \text{FA} - H]^-$ , respectively. The HRMS determined its molecular formula as  $\text{C}_{57}\text{H}_{89}\text{NO}_{16}$  (measd: 1042.6073, calcd: 1042.6108 for  $[M - H]^-$ ). Compared to temsirolimus this composition had

one extra carbon and two extra hydrogen atoms, indicative of a  $\text{CH}_2$  unit. The MS/MS fragmentation of **2a** indicated that the additional 14 Da was located between C-10 and C-14. As can be seen in the MS/MS fragmentation pattern for **2a** (Figure 2), fragment ion **D**,  $m/z$  387, corresponds to the loss of methanol from the component generated by the cleavage of C–C bonds between C-9 and C-10 and between C-27 and C-28. Fragment ion **D** is 14 Da greater than the corresponding ion observed for temsirolimus at  $m/z$  373. Likewise, fragment ion **E**,  $m/z$  248, corresponds to the loss of water from the component generated by the cleavage of C–C bonds between C-1 and C-2 and between C-14 and C-15. Fragment ion **E** is 14 Da greater than the corresponding ion observed for temsirolimus at  $m/z$  234. Combining these results for fragment ions **D** and **E**, the position of the extra methylene unit must be between C-10 and C-14.

The structure of **2a** was elucidated by NMR spectroscopy. The  $^1\text{H}$  and  $^{13}\text{C}$  NMR spectra of **2a** were quite similar to those of temsirolimus.<sup>14</sup> The noticeable difference was in the region typical for methyl group resonances. The disappearance of the C-11 methyl doublet at  $\delta$  0.73 for temsirolimus and the appearance of a methyl triplet at  $\delta$  0.77, which was partially overlapped with the C-35 methyl doublet at  $\delta$  0.78 (Supporting Information), suggested the replacement of the 11-methyl group by an ethyl group at C-11. Detailed analyses of the 1D and 2D NMR data led to the full assignments for **2a**. Specifically, in the HSQC spectrum, the methyl triplet (H-11b) was correlated to an upfield carbon at  $\delta$  11.2 that was assigned to the terminal methyl carbon (C-11b) of the ethyl group. In the HMBC spectrum, the methyl triplet showed two cross-peaks at  $\delta$  22.5 and 41.2, assigned to C-11a and C-11, respectively. An important HMBC correlation observed between the C-11 resonance and the C-10 hydroxyl proton (C-10-OH) at  $\delta$  6.43 secured the location of the ethyl group. The  $^1\text{H}$  and  $^{13}\text{C}$  NMR data for the rest of the

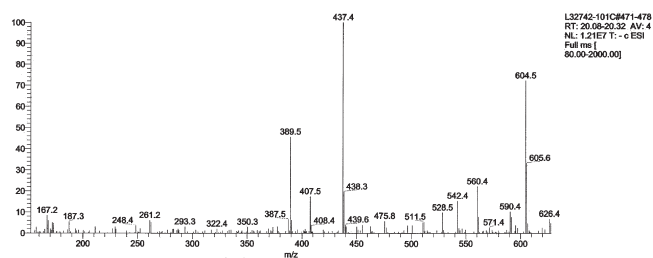
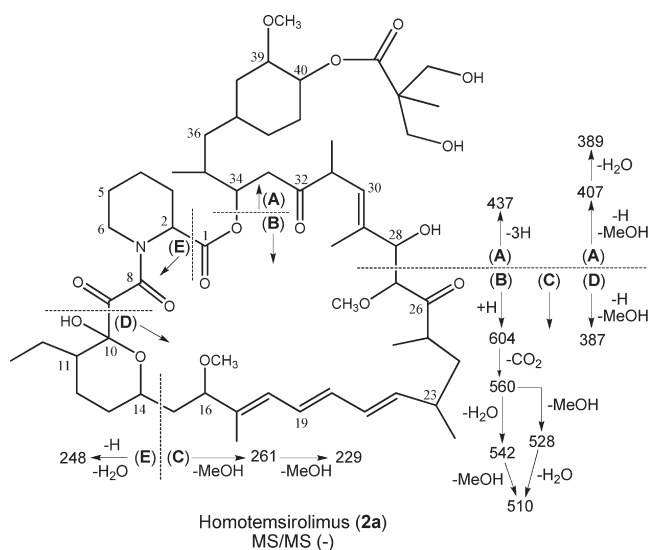


**Figure 2.** MS/MS fragmentation pattern of homotemsirolimus A (2a) in negative ionization mode.

molecule were virtually identical to those of temsirolimus except for the resonances of C-12 at  $\delta$  22.7 and its attached protons. This 3.5 ppm shielding is caused by the  $\gamma$ -effect due to the presence of an additional carbon. The proton and carbon NMR assignments are shown in Table 1.

It should be noted that a definitive assignment for the H-12 methylene protons of **2a** was very challenging due to the correlation with H-11 at  $\delta$  1.81, which was severely overlapped with other protons resonating at around 1.8 ppm in the COSY and TOCSY spectra. Analysis of the HMBC data also failed to unambiguously establish the C-11/C-12 connectivity. The existence of the complex structure as a mixture of *trans* and *cis* rotamers in DMSO at about 9:1 ratio further complicated the assignment.<sup>15</sup> Fortunately, the ROESY spectrum clearly shows the correlations from the hemiketal proton (10-OH) at  $\delta$  6.43 to H-11a at  $\delta$  0.99 and 1.27, H-12<sub>ax</sub> at  $\delta$  1.38, H-6<sub>eq</sub> at  $\delta$  3.44, and H-14<sub>ax</sub> at  $\delta$  4.02, as shown in Figure 3. The correlation between 10-OH and H-12<sub>ax</sub> secured the <sup>1</sup>H and <sup>13</sup>C NMR assignments for the C-12 methylene. This definitive assignment is important since C-12 has been misassigned in a previous publication<sup>15</sup> that assigned C-12 as 31.09 ppm and C-42 as 26.22 ppm, which were later found to be interchanged.<sup>16</sup> A similar mistake was also documented in a paper investigating the biosynthesis of rapamycin using <sup>13</sup>C-labeled precursors where the assignments of the signals of C-12 and C-3, as well as the resonances assigned to C-19 and C-20, were interchanged.<sup>17,18</sup> Because of these misassignments, the authors stated, “Surprisingly, C-12 and C-20 (predicted to be derived from C-1 of acetate) were not significantly enriched, while C-19 (predicted to be derived from C-2 of

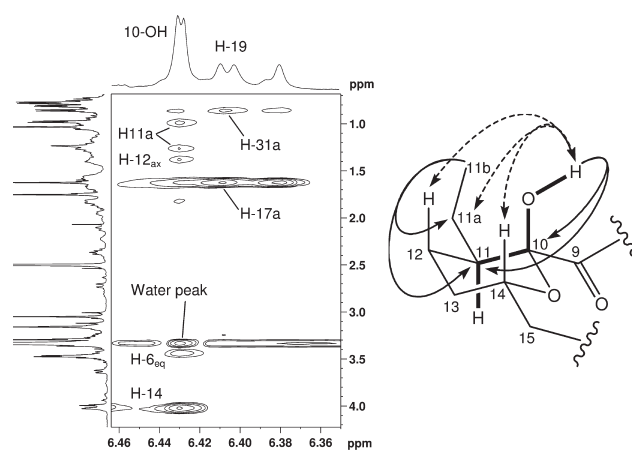


**Figure 3.** Portion of the ROESY spectrum and key 2D NMR correlations for the tetrahydropyran ring moiety of homotemsirolimus A (2a): <sup>4</sup>J COSY correlation/W-coupling (bold bonds), HMBC correlations (plain arrow, proton to carbon), and ROESY correlations (dashed arrows).

acetate) was highly enriched.”<sup>17</sup> These NMR assignments were later revised.<sup>19</sup>

The doublet signal of the hemiketal proton (10-OH) with a coupling constant of 1.5 Hz was attributed to the *W*-coupling as shown in Figure 3. It was correlated to H-11 in the COSY spectrum. The chair conformation for the tetrahydropyran ring was supported by the ROESY data. Thus, the ROESY correlations between 10-OH and H12<sub>ax</sub> between H12<sub>ax</sub> and H14<sub>ax</sub> and between H14<sub>ax</sub> and 10-OH were observed as illustrated in Figure 3. An additional important ROESY correlation can be seen in Figure 3 between the olefinic proton H-19 at  $\delta$  6.41 and methyl protons H-31a at  $\delta$  0.86. This transannular NOE correlation indicated that the backbone conformation of the *trans* rotamer is consistent with the crystal structure of rapamycin.<sup>20</sup> It is worth pointing out that the structural representation presented in the paper reporting the X-ray crystallographic structure of rapamycin<sup>20</sup> is the mirror image of the absolute configuration of rapamycin.<sup>18</sup>

Homotemsirolimus B (2b) was isolated as an amorphous powder. The LC-MS analysis of **2b** revealed its molecule related ions at *m/z* 1061, 1066, 1042, and 1088, corresponding to [M + NH<sub>4</sub>]<sup>+</sup>, [M + Na]<sup>+</sup>, [M - H]<sup>-</sup>, and [M + FA - H]<sup>-</sup>, respectively. The HRMS determined its molecular formula as C<sub>57</sub>H<sub>89</sub>NO<sub>16</sub> (measd: 1042.6108, calcd: 1042.6108 for [M - H]<sup>-</sup>), identical to that of homotemsirolimus A, indicating it also contained an additional methylene unit compared to temsirolimus. The UV spectrum showed that it had an identical absorption curve to temsirolimus, indicating the extra CH<sub>2</sub> group did not affect the chromophore. The MS/MS fragmentation determined that the additional 14 amu was located between C-15 and C-27. In the fragmentation labeled C, the fragments, generated by cleavages at C-14/C-15 and C-27/C-28 with the consecutive loss of two methanols, changed to *m/z* 275 and 243 for **2b** from *m/z* 261 and 229 for temsirolimus, respectively (Supporting Information).

The NMR assignments for **2b** were achieved by interpretation of the 1D and 2D NMR spectra. The carbon chemical shifts were mainly extracted from the 2D spectra owing to the limited quantity of sample. It should be noted that it was extremely difficult to identify each carbon and proton resonance for **2b** because the sample was approximately a 1:1 mixture of homotemsirolimus B and its seco counterpart.<sup>21</sup> Fortunately, the

Table 1. NMR Spectroscopic Data for Homotemsirolimus A (2a), Homotemsirolimus B (2b), and Homotemsirolimus C (2c) in DMSO- $d_6$ 

position	2a		2b		2c	
	$\delta_C$	$\delta_H$ (J in Hz)	$\delta_C$	$\delta_H$ (J in Hz)	$\delta_C$	$\delta_H$ (J in Hz)
1	169.2		169.2		169.2	
2	50.9	4.9S, bd (5.1)	50.7	4.94, d (5.3)	50.8	4.91, bd (5.4)
3	26.4	2.12/1.56	26.4	2.10/1.56	26.7	2.09/1.61
4	20.4	1.67/1.40	20.3	1.66/1.39	20.4	1.66/1.40
5	24.5	1.57/1.29	24.5	1.58/1.26	24.4	1.58/1.28
6	43.5	3.44/3.14	43.4	3.43/3.16	43.5	3.43/3.14
8	167.0		167.2		167.0	
9	198.7		198.7		198.7	
10	99.1		99.0		99.0	
10-OH		6.43, d (1.5)		6.47, d (1.5)		6.46, d (1.5)
11	41.2	1.81	34.8	2.03	34.8	2.03
11a	22.5	1.27/0.99	15.5	0.73, d (6.7)	15.5	0.73, d (6.7)
11b	11.2	0.77, t (7.6)				
12	22.7	1.75/1.38	26.2	1.53	26.2	1.52
13	29.5	1.86/1.15	29.5	1.82/1.16	29.5	1.83/1.19
14	66.4	4.02	66.2	4.00	66.2	4.00
15	40.2	1.84/1.21	40.1	1.87/1.23	40.2	1.83/1.31
16	82.2	3.63, dd (11.7, 1.7)	82.2	3.63, dd (11.5, 1.9)	82.2	3.64, dd (11.7, 2.1)
16-OCH <sub>3</sub>	55.5	3.05, s	55.4	3.05, s	55.5	3.06, s
17	137.9		137.9		137.8	
17a	10.5	1.63, s	10.3	1.63, s	10.8	1.66, s
18	127.0	6.12, d (10.9)	126.9	6.11, d (11.3)	126.8	6.11, d (11.3)
19	127.0	6.41, dd (14.6, 11.3)	127.1	6.41, dd (14.7, 11.3)	127.0	6.44, dd (14.3, 11.5)
20	132.4	6.23, dd (14.6, 10.6)	132.6	6.25, dd (14.7, 10.7)	132.3	6.22, dd (14.3, 10.5)
21	130.4	6.13, dd (14.6, 10.7)	131.8	6.13, dd (15.0, 10.8)	130.2	6.14, dd (14.6, 10.5)
22	139.3	5.46, dd (14.6, 9.6)	137.7	5.41, dd (14.9, 9.7)	139.3	5.50, dd (14.6, 9.4)
23	35.2	2.21, m	42.5	1.96	35.0	2.22, m
23a	21.6	0.98, d (6.5)	28.3	1.36/1.25	21.9	0.98, d (6.5)
23b			11.8	0.81, t (7.5)		
24	39.5	1.41/1.04	37.5	1.39/1.10	39.3	1.44/1.06
25	39.8	2.38	39.2	2.42	39.8	2.48
25a	13.2	0.81, d (6.4)	13.2	0.82, d (6.6)	14.0	0.84, d (6.5)
26	210.3		210.6		210.0	
27	85.4	3.99, d (4.3)	85.4	3.94, d (4.6)	85.8	3.87, d (5.2)
27-OCH <sub>3</sub>	56.9	3.16, s	57.1	3.15, s	57.1	3.15, s
28	75.7	4.02	75.7	4.02, t (4.5)	75.7	4.01
28-OH		5.29, d (4.4)		5.28, d (4.5)		5.25, d (4.6)
29	137.1		137.1		137.7	
29a	13.6	1.75, s	13.5	1.74, s	13.2	1.72, s
30	124.7	5.10, d (10.1)	124.9	5.09, d (10.1)	124.3	5.09, d (10.1)
31	45.3	3.25, dq (10.1, 6.6)	45.2	3.26	52.1	3.16
31a	15.5	0.86, d (6.5)	15.5	0.87, d (6.6)	23.8	1.55/1.19
31b					11.1	0.70, t (7.4)
32	207.6		207.6		207.1	
33	39.7	2.72, dd (17.4, 2.2) 2.36, dd (17.4, 9.0)	39.6	2.74, dd (17.8, 2.3) 2.37	41.3	2.76, bd (18.3) 2.41, dd (18.3, 9.0)
34	73.6	4.99, m	73.5	4.98, m	73.1	5.03, m
35	33.4	1.68	33.3	1.68	33.2	1.71
35a	14.6	0.78, d (6.6)	14.6	0.78, d (6.7)	14.9	0.80, d (6.7)
36	38.1	1.06/0.99	38.0	1.06/0.98	38.1	1.09/1.00
37	32.1	1.34	32.2	1.31	32.1	1.36

Table 1. Continued

position	2a		2b		2c	
	$\delta_C$	$\delta_H$ (J in Hz)	$\delta_C$	$\delta_H$ (J in Hz)	$\delta_C$	$\delta_H$ (J in Hz)
38	35.9	1.95/0.75	35.8	1.94/0.72	35.8	1.97/0.74
39	80.2	3.17	80.2	3.16	80.2	3.17
39-OCH <sub>3</sub>	57.2	3.29, s	57.2	3.29, s	57.3	3.29, s
40	75.8	4.50, ddd (11.3, 9.6, 4.9)	75.7	4.50, ddd (11.3, 9.5, 5.1)	75.8	4.50, ddd (11.1, 9.5, 4.8)
41	29.2	1.83/1.25	29.2	1.79/1.24	29.2	1.83/1.25
42	30.5	1.58/0.94	30.5	1.57/0.94	30.6	1.57/0.93
43	174.2		174.2		174.2	
44	49.9		49.9		49.9	
45	16.8	1.03, s	16.8	1.03, s	16.8	1.03, s
46	63.7	3.47	63.7	3.47	63.7	3.47
46-OH		4.57, t (5.4)		4.56, t (5.4)		4.56, t (5.3)
47	63.6	3.47	63.6	3.47	63.6	3.47
47-OH		4.57, t (5.4)		4.56, t (5.4)		4.56, t (5.3)

signals assigned to the ethyl group for both homotemsirolimus B and its seco counterpart were virtually identical, suggesting the chemical environment of the ethyl group was very similar in both compounds. Therefore, identification of the ethyl group was straightforward from the COSY and HSQC data. In the HMBC spectrum, the methyl triplet at  $\delta$  0.81 (H-23b) showed HMBC correlations to C-23a at  $\delta$  28.3 and C-23 at  $\delta$  42.5. In addition, the olefinic proton H-22 at  $\delta$  5.41 showed correlations to C-23 and C-23a. This result established the position of the ethyl group at C-23. Due to the  $\gamma$ -effect, both C-22 and C-24 resonated at higher field at  $\delta$  137.7 and 37.5, respectively, compared to those of temsirolimus at  $\delta$  139.3 and 39.1. Full assignments of the <sup>1</sup>H and <sup>13</sup>C NMR data for **2b** are listed in Table 1. The seco compound was generated during the sample preparation from evaporation of the large volume of the slightly acidic methanol/water HPLC mobile phase. Later, it was found that formation of the seco byproduct could be avoided by dilution of the methanol/water HPLC solution with acetonitrile followed by removal of the solvents by rotary evaporation and lyophilization.

Homotemsirolimus C (**2c**) was isolated as an amorphous powder. The UV spectrum showed that it had an identical absorption curve to temsirolimus, indicating the extra CH<sub>2</sub> group did not affect the chromophore. The HRMS analysis of **2c** revealed its molecular ions at  $m/z$  1042 and 1102 in the electrospray negative ionization mode, corresponding to  $[M - H]^-$  and  $[M + AA - H]^-$ , respectively. The HRMS determined its molecular formula as C<sub>57</sub>H<sub>89</sub>NO<sub>16</sub>, deduced from its quasi molecular ion  $[M - H]^-$  with  $m/z$  at 1042.6110 corresponding to an ionic formula of C<sub>57</sub>H<sub>88</sub>NO<sub>16</sub> (calcd: 1042.6108). This was consistent with the structure of **2c** (Figure 1), implying its composition also had one more methylene unit than temsirolimus. The MS/MS fragmentation determined that the additional 14 amu was located between C-28 and the esterified carbon C-34. In the MS/MS spectrum (Supporting Information), the fragmentation labeled A showed fragments at  $m/z$  451, 421, and 403, compared to 437, 407, and 389 for temsirolimus. In the southern part of the molecule, labeled fragmentation B, the fragments with  $m/z$  590, 546, 528, 514, and 496 were identical to those of temsirolimus.

The NMR spectroscopic analyses of **2c** determined that it was the 31-ethyl analogue. The <sup>1</sup>H and <sup>13</sup>C NMR spectra of **2c** were quite similar to those of temsirolimus. The noticeable difference was in the methyl region between  $\delta$  1.0 and 0.7 ppm, where there were four methyl doublets at  $\delta$  0.98, 0.84, 0.80, and 0.73 and one

methyl triplet at  $\delta$  0.70 observed for **2c** instead of the five methyl doublets for temsirolimus. The four methyl doublets could be easily assigned to the methyl groups attached at C-23, C-25, C-35, and C-11, respectively, when compared to those of temsirolimus. The lack of the methyl doublet (H-31a) observed at  $\delta$  0.86 for temsirolimus suggested that this group was replaced by an ethyl group at C-31 in **2c**. Assignment of this ethyl group was straightforward from the COSY and HSQC data. Thus, the methyl triplet at  $\delta$  0.70 (H-31b), shown to be directly bonded to a carbon at  $\delta$  11.1 (C-31b) from the HSQC spectrum, showed scalar couplings to two methylene protons at  $\delta$  1.55 (H-31a) and 1.19 (H-31a), which were further correlated to a methine proton at  $\delta$  3.16 (H-31). In the HMBC spectrum, the methyl triplet signal (H-31b) showed two cross-peaks at  $\delta$  23.8 and 52.1, assigned to C-31a and C-31, respectively. In addition, the olefinic proton H-30 at  $\delta$  5.09 showed a correlation in the COSY spectrum to the methine proton H-31, securing the location of the ethyl group at C-31. A correlation in the TOCSY spectrum between the methyl triplet protons H-31b and the olefinic proton H-30 further supported the above assignment. Due to the  $\beta$ -effect, C-31 resonated at lower field,  $\delta$  52.1, for homotemsirolimus C compared to temsirolimus,  $\delta$  45.2. Detailed analyses of the 2D NMR data led to the full assignments for **2c**. The <sup>1</sup>H and <sup>13</sup>C NMR data for the rest of the molecule were virtually identical to temsirolimus. All assignments are listed in Table 1.

Therefore, the "impurity peak at RRT 1.15" was determined to be three temsirolimus analogues, homotemsirolimuses A, B, and C (**2a**, **2b**, and **2c**). Since these analogues cannot be formed as byproducts during the synthetic transformation of rapamycin to temsirolimus, they must be naturally derived from their corresponding rapamycin analogues, homorapamycins A, B, and C (**1a**, **1b**, and **1c**). In fact, a similar late peak of M + 14 amu (RRT 1.31 by HPLC method 4072-103) was detected during the analytical method development for Rapamune (rapamycin). This RRT 1.31 peak was registered as WAY-155618 and characterized as rapamycin plus CH<sub>2</sub> compound(s).<sup>22</sup>

**Biosynthetic Origin.** On the basis of our knowledge of the biosynthetic pathway, the biogenesis of homorapamycins A, B, and C (**1a**, **1b**, and **1c**) can be established. The biosynthetic pathway of rapamycin begins with a cyclic C<sub>7</sub> unit derived from the shikimic acid pathway,<sup>23</sup> and then the long polyketide chain portion (C-8 to C-35) is built up from the condensation of seven

**Table 2. mTOR Kinase Assay (IC<sub>50</sub>'s) and Cell Assay (IC<sub>50</sub>'s) Results of Homotemsirolimus A (2a), Homotemsirolimus B (2b), Homotemsirolimus (2c), and Temsirolimus (2)**

	mTOR and cell data, IC <sub>50</sub> (μM)			
	mTOR kinase assays <sup>a</sup>		3 day cell growth data	
	plate 1	plate 2	LNCap	MDA468
homotemsirolimus A	1.8	2.8	0.0025	0.001
homotemsirolimus B	2.5	3.7	0.013	0.005
homotemsirolimus C	2.1	4	0.008	0.005
temsirolimus (control)	1.76	1.76	0.0005–0.001	0.008

<sup>a</sup>mTOR kinase assay in the absence of FKBP12 as described by Shor et al.<sup>27</sup>

acetate and seven propionate units.<sup>17</sup> Apparently, homorapamycins A, B, and C are produced by incorporating a butyrate unit (ethylmalonyl-CoA) into the rapamycin's macrolide core at various locations instead of a propionate (methylmalonyl-CoA). The ethyl instead of methyl "side chain" is a possible biosynthetic shunt product. In fact, it may be possible that any one of the seven methyl side chains could exist as an ethyl side chain due to this misincorporation. The directed biosynthesis of novel rapamycin analogues has mainly focused on feeding studies with modifications to the 4,5-dihydroxycyclohex-1-ene carboxylic acid starter unit<sup>24</sup> and modified pipercolates or proline as end units.<sup>25,26</sup> However, little has been done on modification of the polyketide chain. The discovery of homorapamycins A, B, and C may open a new avenue to produce novel members of the rapamycin class of compounds.

**Biological Activity.** Rapamycin and temsirolimus exhibit a classical FKBP12-dependent mTOR inhibition (IC<sub>50</sub> values in the single digit nanomolar range) as well as the recently characterized FKBP12-independent mTOR inhibition (IC<sub>50</sub> values in the 1–2 μM), reflecting direct binding of the compound to the FRB domain.<sup>27</sup> While the FKBP12-dependent mTOR inhibition by rapamycins generally leads to a selective and moderate reduction of tumor cell growth, the FKBP12-independent rapamycin action correlates with a more broad and profound antitumor activity that is relevant to its anticancer efficacy. The temsirolimus analogues, **2a**, **2b**, and **2c**, were assayed for mTOR kinase inhibition without FKBP12, achieving mean IC<sub>50</sub> values of 2.3, 3.1, and 3.1 μM, respectively (Table 2). In the proliferation assays of rapamycin-sensitive prostate cancer LNCap and breast cancer MDA468 cells, **2a**, **2b**, and **2c** potently inhibited both cell lines with IC<sub>50</sub> values in the single digit nanomolar range (Table 2). These data indicate that the biochemical and cellular mTOR inhibition potencies for **2a**, **2b**, and **2c** are in the same range as those of rapamycin and temsirolimus. It can thus be concluded that these novel analogues may be useful in treating mTOR-related diseases such as cancer.

## EXPERIMENTAL SECTION

**General Experimental Procedures.** Electrospray mass spectra were measured on a Waters micromass ZQ mass spectrometer. LC-MS and source fragmentations were recorded on a Finnigan LCQ LC-MS system. MS/MS data and accurate mass measurements were conducted on an Applied Biosystems PE SCIEX QSTAR PULSAR *i* quadrupole time-of-flight tandem mass spectrometer with a TurboIonSpray source.

The collision energy used for getting the MS/MS/CID spectrum was set at 35 eV. NMR spectra were recorded on a Bruker DRX 500 spectrometer with a QNP probe or a Bruker DRX 600 equipped with a 5 mm TXI z-gradient probe in deuterated solvents. <sup>1</sup>H and <sup>13</sup>C chemical shifts were measured in parts per million relative to partially deuterated solvent peaks of DMSO-*d*<sub>6</sub> at δ 2.50 and 39.5 for <sup>1</sup>H and <sup>13</sup>C NMR signals, respectively. <sup>1</sup>H–<sup>1</sup>H coupling constants were measured from 1D proton spectra and are given in hertz. A typical NMR data set measured for a compound included carbon, DEPT-135, proton, COSY, TOCSY, HSQC, HMBC, NOESY and/or ROESY, and HSQC-TOCSY spectra. All 2D experiments were run nonspinning.

**HPLC Systems.** A Hewlett-Packard 1100 M LC system with diode array detection and a Finnigan LCQ LC-MS system employing a YMC-ODS-A reversed-phase column (5 μm, 4.6 × 150 mm or 4.6 × 250 mm) were used for analysis of temsirolimus API samples and preparative and semipreparative HPLC fractions. Preparative HPLC separations were achieved using a Phenomenex column (C18, 250 × 50 mm), and semipreparative HPLC was performed with a Varian Inertsil 5u ODS-3 column (250 × 10 mm). Fractions from semipreparative columns were generally collected using an ISCO Foxy fractional collector and monitored by analytical HPLC or LC-MS. All solvents used were obtained from EM Science or J. T. Baker, Inc., and were of the highest commercially available purity.

**Isolation.** Temsirolimus API, batch OM7612 (2 g), was dissolved in a mixture of 20 mL of acetonitrile and dimethyl sulfoxide at a ratio of 4:1, and the solution was then loaded onto a reversed-phase HPLC column (Phenomenex, 250 × 50 mm, two injections). The column was washed with an isocratic solvent system consisting of 70% acetonitrile and 30% water for 30 min, followed by a linear gradient of 70–90% acetonitrile in water over 20 min, and then isocratic elution again with 90% acetonitrile for 20 min at a flow rate of 50 mL/min with UV detection at 275 nm. Fractions were collected according to peaks or time intervals. The collected samples were analyzed by analytical HPLC and/or LC-MS using a model HP 1100 system and/or a Thermoquest-Finnigan LCQ-DECA ion trap mass spectrometer. The fraction collected from 31 to 38 min (Supporting Information) contained the RRT 1.15 compounds and was subjected to further separations.

The above fraction was then purified by semipreparative reversed-phase HPLC (Varian Inertsil 5u ODS-3 column, 250 × 10 mm) using an isocratic elution of 65% acetonitrile/35% water at a flow rate of 4 mL/min to yield the relatively pure RRT 1.15-containing fraction (36.6 min, 19 mg, Supporting Information).

The pure RRT 1.15-containing fraction was subjected to another round of separation by reversed-phase HPLC (Varian Inertsil 5u ODS-3 column, 250 × 10 mm) using an isocratic elution of 77% methanol/23% water at a flow rate of 4 mL/min to give relatively pure **2a** (42.5–45.5 min, 5.6 mg) and a fraction with the second major component **2b** enriched (45.5–49.0 min, 7.0 mg). A small amount of **2c** was also obtained at retention time 40.7 min from this HPLC run. Final purification of the second major component-containing sample was achieved by reversed-phase HPLC (Varian Inertsil 5u ODS-3 column, 250 × 10 mm) using an isocratic elution of 74% methanol/26% water at a flow rate of 4 mL/min to yield **2b** (82–86 min, 2.6 mg).

To isolate a sufficient amount of **2c**, additional API (batch RB3609, 5 g) was subjected to the above isolation procedures to yield the temsirolimus RRT 1.15 fraction. This batch contained a lower amount of the RRT 1.15 impurity. A final separation by reversed-phase HPLC (Varian Inertsil 5u ODS-3 column, 250 × 10 mm) using an isocratic elution of 75% methanol/25% water at a flow rate of 4 mL/min yielded pure **2c** (52–58 min, 2 mg). Small quantities of **2a** and **2b** were also obtained.

**Biological Assays.** Recombinant mTOR kinase activity was measured with vehicle and various doses of **2a**, **2b**, and **2c** without FKBP12.<sup>27</sup> Percent inhibition relative to control was plotted for

determination of IC<sub>50</sub> values. LNCap (ATCC: CRL-1740) and MDA468 (ATCC: HTB-132) cells were obtained from American Type Culture Collection and maintained according to standard culture methods. Cells were plated in 96-well culture plates for 24 h, then exposed to vehicle and various doses of **2a**, **2b**, and **2c** for 3 days, after which viable cell densities were determined by MTS assay using an assay kit purchased from Promega Corp. (Madison, WI). Percent inhibition relative to control was plotted for determination of IC<sub>50</sub> values.

## ■ ASSOCIATED CONTENT

Supporting Information. This material is available free of charge via the Internet at <http://pubs.acs.org>.

## ■ AUTHOR INFORMATION

### Corresponding Author

\*Tel: 860-715-6823. Fax: 860-686-5233. E-mail: [fangming.kong@pfizer.com](mailto:fangming.kong@pfizer.com).

### Notes

Wyeth was acquired by Pfizer on October 16, 2009.

## ■ ACKNOWLEDGMENT

The authors would like to thank N. C. Ocampo for assistance in confirming RRT values and R. Tsao for HRMS measurements. The authors also wish to thank M. E. Ruppen, G. Schlingmann, R. Tsao, and T. J. Callaghan for helpful discussions.

## ■ REFERENCES

- (1) (a) Vézina, C.; Kudelski, A.; Sehgal, S. N. *J. Antibiot.* **1975**, *28*, 721–726. (b) Sehgal, S. N. *Transplantation Proceedings* (2003), *35*(3A).
- (2) Sehgal, S. N.; Baker, H.; Vézina, C. *J. Antibiot.* **1975**, *28*, 727–732.
- (3) (a) Martel, R. R.; Klicius, J.; Galet, S. *Can. J. Physiol. Pharmacol.* **1977**, *55*, 48–51. (b) Calne, R. Y.; Collier, D. S.; Lim, S.; Pollard, S. G.; Samaan, A.; White, D. J. G.; Thiru, S. *Lancet* **1989**, *334*, 227.
- (4) Pritchard, D. I. *Drug Discovery Today* **2005**, *10*, 688–691.
- (5) Choi, J.; Chen, J.; Schrieber, S. L.; Clardy, J. *Science* **1996**, *273*, 239–241.
- (6) Sousa, J. E.; Costa, M. A.; Abizaid, A.; Abizaid, A. S.; Feres, F.; Pinto, I. M. F.; Seixas, A. C.; Staico, R.; Mattos, L. A.; Sousa, A. G. M. R.; Falotico, R.; Jaeger, J.; Popma, J. J.; Serruys, P. W. *Circulation* **2001**, *103*, 192–195.
- (7) Abraham, R. T. *Curr. Top. Microbiol. Immunol.* **2004**, *279*, 299–319.
- (8) Harrison, D. E.; Strong, R.; Sharp, Z. D.; Nelson, J. F.; Astle, C. M.; Flurkey, K.; Nadon, N. L.; Wilkinson, J. E.; Frenkel, K.; Carter, C. S.; Pahor, M.; Javors, M. A.; Fernandez, E.; Miller, R. A. *Nature* **2009**, *460*, 392–396.
- (9) Punt, C. J. A.; Boni, J.; Brunsch, U.; Peters, M.; Thielert, C. *Ann. Oncol.* **2003**, *14*, 931–937.
- (10) Kirchner, G. I.; Meier-Wiedenbach, L.; Manns, M. P. *Clin. Pharmacokinet.* **2004**, *43*, 83–95.
- (11) (a) Palaparthi, R.; Pradhan, R.; Chan, J.; Wang, Q.; Ji, Q.; Achari, R.; Chira, T.; Schwartz, L. B.; O'Dea, R. *Clin. Drug Invest.* **2005**, *25*, 491–498. (b) Karyekar, C. S.; Pradhan, R. S.; Freeney, T.; Ji, Q.; Edeki, T.; Chiu, W.; Awni, W. M.; Locke, C.; Schwartz, L. B.; Granneman R. G.; O'Dea, R. *J. Clin. Pharmacol.* **2005**, *45*, 910–918. (c) Chen, Y. W.; Smith, M. L.; Sheets, M.; Ballaron, S.; Trevillyan, J. M.; Burke, S. E.; Rosenberg, T.; Henry, C.; Wagner, R.; Bauch, J.; Marsh, K.; Fey, T. A.; Hsieh, G.; Gauvin, D.; Mollison, K. W.; Carter, G. W.; Djuric, S. W. *J. Cardiovasc. Pharmacol.* **2007**, *49*, 228–235.
- (12) Mita, M. M.; Mita, A. C.; Chu, Q. S.; Rowinsky, E. K.; Fetterly, G. J.; Goldston, M.; Patnaik, A.; Mathews, L.; Ricart, A. D.; Mays, T.; Knowles, H.; Rivera, V. M.; Kreisberg, J.; Bedrosian, C. L.; Tolcher, A. W. *J. Clin. Oncol.* **2008**, *26*, 361–367.
- (13) Ruan, B.; Pong, K.; Jow, F.; Bowlby, M.; Crozier, R. A.; Liu, D.; Liang, S.; Chen, Y.; Mercado, M. L.; Feng, X.; Bennett, F.; vonSchack, D. McDonald, M.; Zaleska, M.; Wood, A.; Reinhart, P.; Magolda, R. L.; Skotnicki, J.; Pangalos, M. N.; Koehn, F. E.; Carter, G. T.; Abou-Gharbia, M. Graziani, E. I. *Proc. Natl. Acad. Sci. U. S. A.* **2008**, *105*, 33–38.
- (14) Callaghan, T. J. *Temsirolimus Reference Standard Qualification and Proof of Structure*; Wyeth Research Internal Reports RPT-63432, Version 1.0, 2005.
- (15) Kessler, H.; Haessner, R.; Shuler, W. *Helv. Chim. Acta* **1993**, *76*, 117–130.
- (16) Pagano, T. G. *Magn. Reson. Chem.* **2005**, *43*, 174–175.
- (17) Paiva, N. L.; Demain, A. L.; Roberts, M. F. *J. Nat. Prod.* **1991**, *54*, 167–177.
- (18) Findlay, J. A.; Radics, L. *Can. J. Chem.* **1980**, *58*, 579–590.
- (19) McAlpine, J. B.; Swanson, S. J.; Jackson, M.; Whittern, D. N. *J. Antibiot.* **1991**, *44*, 688–689.
- (20) Swindells, D. C. N.; White, P. S.; Findlay, J. A. *Can. J. Chem.* **1978**, *56*, 2491–2492.
- (21) Wang, C. P.; Chan, K. W.; Schiksnis, R. A.; Scatina, J.; Sisenwine, S. F. *J. Liq. Chromat.* **1994**, *17*, 3383–3392.
- (22) Longfellow, C. *Proof of Structure for WAY-155618, a Process Impurity in Sirolimus*; Wyeth Research Internal Reports 38726, 2000.
- (23) Schwecke, T.; Aparicio, J. F.; Molnár, I.; König, A.; Khaw, L. E.; Haydock, S. F.; Oliynyk, M.; Caffrey, P.; Cortés, J.; Lester, J. B.; Böhm, G.; Staunton, J.; Leadlay, P. F. *Proc. Natl. Acad. Sci. U. S. A.* **1995**, *92*, 7839–7843.
- (24) Lowden, P. A. S.; Böhm, G.; Metcalfe, S.; Staunton, J.; Leadlay, P. F. *ChemBioChem* **2004**, *5*, 535–538.
- (25) Graziani, E. I.; Ritacco, F. V.; Summers, M. Y.; Zabriskie, M.; Yu, K.; Bernan, V. S.; Greenstein, M.; Carter, G. T. *Org. Lett.* **2003**, *5*, 2385–2388.
- (26) Khaw, L. E.; Böhm, G.; Metcalfe, S.; Staunton, J.; Leadlay, P. F. *J. Microbiol.* **1998**, *180*, 809–814.
- (27) Shor, B.; Zhang, W. G.; Toral-Barza, L.; Lucas, J.; Abraham, R. T.; Gibbons, J.; Yu, K. *Cancer Res.* **2008**, *68*, 2934–2943.